Bottom-Up Assembly of Single-Domain Titania Nanosheets on (1 × 2)-Pt(110)

Tommaso Orzali,[1,2] Maurizio Casarin,[1,2] Gaetano Granozzi,[1,2] Mauro Sambi,[1,2,*] and Andrea Vittadini[1,2,3,†]

[1]*Department of Chemical Sciences, University of Padova, Via Marzolo 1, I-35131 Padova, Italy*
[2]*INSTM, Via Marzolo 1, I-35131 Padova, Italy*
[3]*ISTM-CNR, Via Marzolo 1, I-35131 Padova, Italy*

(Received 18 July 2006; published 9 October 2006)

A bottom-up route towards the synthesis of titania nanosheets is explored, alternative to the exfoliation of layered titanates. Nanosheets are assembled from the constituent elements and epitaxially matched to a suitable substrate: (1 × 2)-Pt(110). Their basic lepidocrocite structure is modulated at the nanoscale due to coincidence with the substrate. Density functional calculations reveal the structure details of the nanosheet, which is also shown to be in close relationship with a (001)-oriented anatase bilayer.

DOI: 10.1103/PhysRevLett.97.156101 PACS numbers: 68.65.−k, 61.14.Qp, 68.37.Ef, 68.43.Bc

Great interest has been aroused in recent years by the so-called inorganic nanosheets, which consist in two-dimensional (2D) crystallites obtained by exfoliation of layered compounds via soft-chemical procedures [1]. Nanosheets can be viewed as a new class of inorganic macromolecules whose peculiar properties are related to size quantization arising from the subnanometer thickness. Among them, titania nanosheets, obtained by delamination of layered titanates, represent an appealing category of 2D semiconductors [2]. The intrinsically Ti-defective quasi-TiO_2 crystallites have a thickness (~0.7 nm) in the molecular range, opposed to lateral dimensions ranging from several hundred nanometers to several micrometers [3]. Their sharp optical absorption peak is considerably blueshifted with respect to bulk TiO_2 [3], and they are, in general, expected to achieve advanced functions such as unidirectional electron or energy transfer, improved photocatalytic activity, and higher photovoltaic efficiency due to reduced electron-hole recombination rates [4,5]. Moreover, organic-inorganic nanocomposites have been obtained by using the nanosheets as building blocks in multilayer assemblies [6], and the synthesis of titania nanotubes by rolling TiO_2 nanosheets has been reported [7].

Such a promising material has prompted many efforts in elucidating its structure-properties relationships. Its structural features have been characterized by means of transmission electron microscopy-based electron diffraction [3], in-plane x-ray diffraction [8], and x-ray absorption fine structure [9]. All techniques yield the picture of a 2D crystal which basically is a double layer of octahedrally coordinated Ti cations arranged periodically in the sheet plane, with a rectangular unit cell of 0.38 nm × 0.30 nm [see Fig. 3(b)]. This arrangement is very similar to the structure of individual lamellae in the stacked parent titanate, whose orthorhombic 3D unit cell is of the lepidocrocite type [10]. Density functional theory (DFT) calculations confirm the experimentally derived structure [4].

So far, the top-down approach consisting in the exfoliation of 3D stacked titanates has been the only known way of producing titania nanosheets. In addition, the structural properties just discussed are obtained as an average over many randomly oriented nanosheet units; local properties at the atomic scale of a single sheet obtained by delamination are more elusive to be tackled experimentally.

In this Letter, we show that single-domain, epitaxial lepidocrocite nanosheets can be produced *ab ovo* from the constituent elements (titanium and molecular oxygen) in an *e*-beam deposition experiment in ultrahigh vacuum (UHV) on a suitable substrate: (1 × 2)-Pt(110) in the present case. Surface science tools can then be applied to investigate their structural properties on the atomic scale. Moreover, DFT calculations reveal that a lepidocrocite nanosheet can be thought of as deriving from an anatase (001) bilayer through a simple structural rearrangement, thereby shedding some light into the lepidocrocite-anatase structural transition observed in some experiments [7,11].

TiO_x films have been grown in an UHV preparation chamber at a base pressure of 5×10^{-9} Pa. The Pt(110) single crystal was prepared by argon ion sputtering (kinetic energy, KE = 2 keV) and annealing at $T = 970$ K, followed by cooling in oxygen ($pO_2 = 5 \times 10^{-3}$ Pa) down to 700 K. The cleaning cycles were repeated until a well ordered (1 × 2) reconstructed surface was obtained, as judged by low energy electron diffraction (LEED). The platinum substrate was chosen because it is known to favor coincidence or even incommensurate titania overlayers [e.g., on Pt (111) (Ref. [12]) and Pt (100) (Ref. [13])]; i.e., the overlayer-substrate interactions are relatively weak, so that intralayer interactions are decisive to determine the structural habit of the ultrathin film. The twofold symmetric surface orientation was chosen in order to act as a template for single-domain growth of an overlayer with the same symmetry. This is further favored by the (1 × 2) missing-row reconstruction of Pt (110) (Ref. [14]) with its highly anisotropic corrugation: The surface is atomically smooth along the $[1\bar{1}0]$ close-packed direction, while it shows alternating ridges and troughs along the reconstructed [001] azimuth. Ti was reactively deposited at room temperature (RT) by means of an *e*-beam evaporator in an oxygen partial pressure of 1×10^{-4} Pa. A postan-

nealing treatment at 700 K followed by cooling down in oxygen ($pO_2 = 1 \times 10^{-4}$ Pa) improves the long-range order of the resulting titania layer and leads to the complete oxidation of Ti [12].

Scanning tunneling microscopy (STM) data were obtained at RT by means of an Omicron variable temperature STM. X-ray photoelectron diffraction (XPD) 2π plots were collected for Ti $2p$ (KE = 1027 eV) and O $1s$ (KE = 956 eV) photoelectrons. The analysis of XPD experimental data has been accomplished with the aid of single scattering cluster–spherical wave (SSC-SW) simulations [15]. DFT calculations were performed using the Perdew-Burke-Ernzerhof exchange-correlation functional [16] and Vanderbilt ultrasoft pseudopotentials [17]. A total of 6, 12, and 10 valence electrons were explicitly considered for O, Ti, and Pt atoms, respectively. The smooth part of the wave function was expanded in plane waves, with a KE cutoff of 25 Ry, while the cutoff for the augmented electron density was 200 Ry. This setup was tested for titania bulk and surface systems [18]. All slab models were built by assuming the theoretical ($a = 0.3957$ nm) Pt lattice constant and by including 5 Pt atomic layers. Only the upper part of the slab was used to simulate the surface, while Pt atoms belonging to the two bottom layers were kept fixed in their bulk positions. Surface Brillouin zones were sampled with the Monkhorst-Pack scheme [19]. The structure and the surface energies of the clean (1×1)- and (1×2)-reconstructed Pt (110) surfaces were found to be in good agreement with previous DFT calculations [20]. Simulated STM images were obtained within the Tersoff-Hamann approach [21].

Figures 1(a) and 1(b) show a large scale (62 nm × 62 nm) and a high resolution (13.7 nm × 13.7 nm) STM image of a fully wetting titania overlayer deposited on (1×2)-Pt(110), respectively. The film thickness corresponds to ~2 monolayers (ML) of anatase (001) [22], as determined by quartz thickness monitor calibrations. A regular array of dark stripes parallel to the [001] substrate direction, whose contrast is bias-independent, is clearly visible in both images. The apparent stripe depth is 0.06 ± 0.01 nm with respect to the adjacent brighter areas. The average stripe separation amounts to 3.9 nm along the $[1\bar{1}0]$ substrate direction, corresponding to 14 substrate unit cell parameters [the $[1\bar{1}0]$ unit vector length for Pt (110) is $a = 0.2775$ nm], although local deviations from this value are observed, which are responsible for the slightly wavy appearance of the stripes. The high resolution images [Figs. 1(b)–1(d)] also evidence a less pronounced corrugation of the overlayer along the [001] substrate direction with a step of 1.6 nm, corresponding to 4 substrate unit cell parameters [the [001] unit vector length for unreconstructed Pt (110) is $b = 0.392$ nm]. Local deviations from the ×4 periodicity are frequently observed and appear as ×3 or ×5 "defects." The corrugation of the ×4 superstructure along [001] is strongly bias-dependent and, hence, due to a large extent to electronic rather than topographic effects: compare Figs. 1(b)–1(d), measured at different bias values.

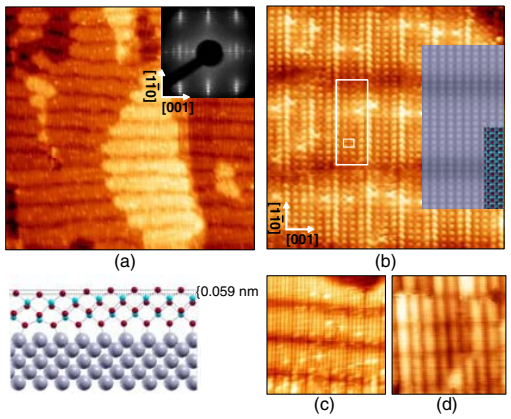

FIG. 1 (color online). (a) Large area STM image (62 nm × 62 nm; bias voltage = 0.48 V; $I_T = 1.4$ nA) of a single-domain lepidocrocite nanosheet on (1×2)-Pt(110). The central brighter area is separated from the lower terrace by a substrate monoatomic step. Inset: (14×4) LEED pattern. (b) High resolution STM image (13.7 nm × 13.7 nm; bias voltage = 0.28 V; $I_T = 1.65$ nA) of the nanosheet. The overlayer (superstructure) unit cell is indicated by the small (large) rectangle. Inset: Tersoff-Hamann simulation of the STM image with superimposed solid sphere model (see text) (oxygen: dark gray/red, titanium: light gray/blue). Dark stripes along [001] are due to overlayer bending toward the substrate (see the interface side view in the [001] plane, lower left corner; Pt: large, gray). (c),(d) High resolution STM images of the nanosheet. (13.6 nm × 13.6 nm; bias voltage = 0.42 V; $I_T = 0.9$ nA and 18.0 nm × 18.0 nm; bias voltage = 1.80 V; $I_T = 1.0$ nA).

In summary, the overall periodicity of the selvedge is (14×4) [see the larger rectangular unit cell in Fig. 1(b)], as confirmed by the LEED pattern reported as an inset in Fig. 1(a). The atomically resolved image [Fig. 1(b)] also reveals the overlayer unit cell, which is a rectangle of 0.30 ± 0.01 nm × 0.39 ± 0.01 nm: Unit vector lengths are both very close to the in-plane lattice parameters for lepidocrocite nanosheets reported in the literature [3,4,8,9]. The ×14 coincidence along $[1\bar{1}0]$ is obtained by matching 13 overlayer to 14 substrate unit cells. The overlayer appears to be strained along the Pt [001] direction (+3.1%) with respect to the unsupported nanosheet, in order to match the substrate lattice parameter.

DFT calculations were first carried out on simple models made by imposing a perfect matching along Pt $[1\bar{1}0]$ between a (strained) lepidocrocite overlayer and the substrate, represented both as an unreconstructed and as a (1×2)-reconstructed Pt (110) surface. These calculations showed that: (i) interface structures where the bridging oxygens of the film facing the substrate sit on top of the surface Pt atoms are favored; (ii) in the presence of the lepidocrocite film, the dereconstruction of (1×2) to (1×1) Pt (110) is energetically favored [by 0.3 eV/(1×1)]. On this basis, we built a more realistic (14×1) model of the interface by placing an overlayer made of 13 lepidocro-

cite unit cells on top of a substrate made of 14 unit cells of (1×1)-Pt(110). The starting geometry was obtained by aligning the rows formed by the bottom bridging oxygens of the overlayer with the $[1\bar{1}0]$ Pt rows of the support. Because of the smaller perturbation it induces in the structure of the supported ultrathin film with respect to the isolated lepidocrocite nanosheet, we did not try to model the $\times 4$ reconstruction along [001] at the present stage, in order to keep the size of the calculations within manageable limits [23]. The results of the DFT optimization show that the ability of the overlayer to induce the Pt(110) dereconstruction is now substantially reduced: The net energy gain becomes tiny (0.01 eV/1×1). It cannot be excluded that the $\times 4$ reconstruction along [001] represents a more efficient route to energy minimization with respect to the dereconstruction. In fact, STM images of small oxide islands partially covering (1×2) terraces (not displayed) show no signs of the Pt mass transport close to the islands required for the dereconstruction. On the structural side, DFT results indicate that the lepidocrocite overlayer indeed develops a coincidence superstructure along the substrate close-packed direction. The coincidence points appear as a periodic bending of the overlayer towards the substrate (see the side view model in Fig. 1), resulting in a physical corrugation of 0.059 nm, in close agreement with the STM data. The Tersoff-Hamann simulation of the surface based on the DFT model is reported in Fig. 1(b) (inset). Both the 0.30 nm $\times$ 0.39 nm unit cell and the dark stripes corresponding to the coincidence are well reproduced. Contrary to the usual experience, the bright protrusions detected at positive bias values are related to oxygen rather than to titanium atoms, as evidenced by the solid sphere model superimposed on the STM simulation.

In summary, STM data are in agreement with the in-plane lattice parameters of the topmost atomic layer of the supported oxide and with the coincidence along $[1\bar{1}0]$, as generated by the DFT optimization. In order to further confirm the DFT model, a test on the vertical atomic stacking in the ultrathin film has been performed by means of XPD measurements. O 1s and Ti 2p XPD 2π plots from the titania overlayer (Fig. 2) have been acquired in the polar angle range $28° \leq \theta \leq 66°$ (with respect to the sample normal), i.e., in the range where the main forward scattering (FS) events are expected for a lepidocrocite nanosheet. Actually, XPD in the FS regime (at photoelectron KE close to 1000 eV) provides a direct fingerprint of the local atomic arrangement surrounding each emitter: The main intensity maxima correspond to interatomic directions and give information regarding the atomic stacking in three dimensions [15,24]. The SSC-SW simulations of XPD 2π plots based on the DFT model are also reported in Fig. 2. All Ti and O atoms along the coincidence period have been explicitly considered as photoelectron emitters, in order to include in the simulations the variation of the local structural environment around each emitter caused by the corrugation profile. The fit of the theoretical to experimental XPD data is excellent, thereby confirming the lepidocrocite structure of the titania ultrathin film.

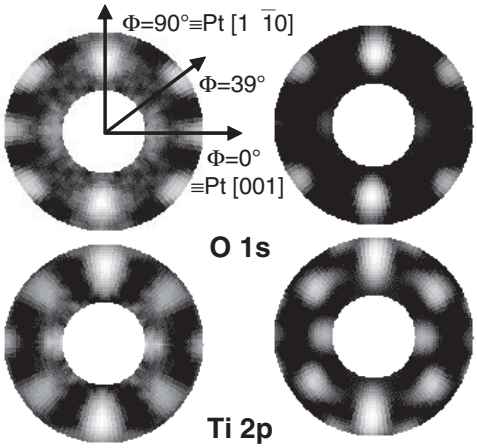

FIG. 2. Experimental XPD 2π plots (left) and SSC-SW simulations based on the DFT model (right) of Ti 2p and O 1s core levels from a lepidocrocite nanosheet on (1×2)-Pt(110). Intensity: white, maximum; black, minimum.

The existence of unsupported lepidocrocite nanosheets in colloidal suspensions suggests that the structure assumed by titania bilayers on Pt (110) [and also on Pt (111) in certain conditions [12,25]] is not interface-stabilized, at variance with what has been observed for other oxide ultrathin phases on metallic substrates [26]. In fact, DFT calculations show that an isolated lepidocrocite nanosheet is the most stable 2D titania phase, irrespective of the presence of a substrate. Consider the anatase bulk

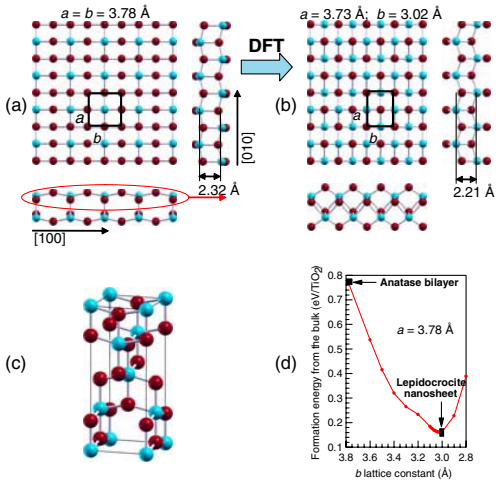

FIG. 3 (color online). (a) Top and side views of an unsupported anatase (001) bilayer (dark gray/red: oxygen; light gray/blue: titanium). (b) Top and side views of an unsupported lepidocrocite nanosheet, obtained from (a) by sliding the upper ML with respect to the lower one by half a unit cell along [100] [as indicated by the ellipse in (a); see text]. (c) Bulk unit cell of anatase TiO_2. (d) DFT formation energy from the bulk vs the lattice parameter along [100] for the (a) $\rightarrow$ (b) structural transition.

unit cell reported in Fig. 3(c). Because of the presence of a fourfold improper rotation axis, the upper half of the unit cell is the mirror image of the lower half, rotated by $\pi/2$. The rotoinversion point is the Ti cation at the center of the unit cell. This symmetry operation forces anatase slabs three or more layers thick to adopt a square unit cell in the (001) plane. However, when the anatase (001) slab thickness is reduced to a single bilayer [see Fig. 3(a)], this constraint is lifted. When both the cell and the internal parameters are freely allowed to relax, DFT calculations show that an anatase (001) bilayer spontaneously transforms into a lepidocrocite nanosheet [Fig. 3(b)], by simply sliding the upper atomic layer with respect to the lower one by half a unit cell along the [100] direction. This involves a shortening of the related unit cell parameter from 0.38 to 0.30 nm and a substantial energy gain: The lepidocrocite nanosheet is stabilized by 1.24 eV with respect to the anatase bilayer and turns out to be only marginally less stable (by 0.16 eV/TiO_2) than bulk anatase [Fig. 3(d)]. This means that it is the reduced dimensionality of the overlayer, rather than the interaction with the substrate, which stabilizes the lepidocrocite structure. Specific interface interactions account for weaker effects only, which show up in the form of the (14×4) reconstruction.

In conclusion, a novel bottom-up route to the production of titania nanosheets has been explored, alternative to layered titanates exfoliation. Single-domain epitaxial nanosheets can be obtained by *e*-beam evaporation in an oxidative atmosphere in UHV conditions on (1×2) Pt (110) and characterized down to the atomic level by means of LEED, XPD, and STM measurements. In addition, DFT calculations evidence the tight relationship between an anatase (001) bilayer and a lepidocrocite nanosheet and, therefore, shed some light into the lepidocrocite-to-anatase structural transitions observed when superimposed nanosheets are heated at 800 °C [11] or when they are rolled into anatase nanotubes and nanorods [7]. This study discloses new perspectives in the investigation of the surface properties and of the chemical reactivity of titania nanosheets.

This work has been funded by the European Community through the STRP project NanoChemSens within the Sixth Framework Programme (Contract No. STRP 505895-1), by the Italian Ministry of Instruction, University and Research (MIUR) through Fund No. PRIN-2005, project title: ''Novel electronic and chemical properties of metal oxides by doping and nanostructuring,'' and by the University of Padova, through Grant No. CPDA038285. We acknowledge a computer time grant from CINECA (Bologna, Italy) and INSTM (Firenze, Italy) under the ''Super-Progetti di calcolo'' program. All the DFT calculations have been done with PWSCF, a code included in the QUANTUM-ESPRESSO package [27]. Graphics were generated by XCRYSDEN [28].

*Corresponding author.
Electronic address: mauro.sambi@unipd.it
†Corresponding author.
Electronic address: andrea.vittadini@unipd.it

[1] A. J. Jacobson, Mater. Sci. Forum **152–153**, 1 (1994).
[2] T. Sasaki *et al.*, J. Am. Chem. Soc. **118**, 8329 (1996).
[3] T. Sasaki and M. Watanabe, J. Phys. Chem. B **101**, 10 159 (1997).
[4] H. Sato *et al.*, J. Phys. Chem. B **107**, 9824 (2003).
[5] N. Sasai *et al.*, J. Phys. Chem. B **109**, 9651 (2005); X. G. Xu *et al.*, Phys. Rev. B **73**, 165403 (2006).
[6] T. Sasaki *et al.*, Chem. Mater. **13**, 4661 (2001).
[7] F. Wang *et al.*, Chem. Lett. **34**, 1238 (2005).
[8] T. Sasaki *et al.*, J. Phys. Chem. B **105**, 6116 (2001).
[9] K. Fukuda *et al.*, J. Phys. Chem. B **108**, 13 088 (2004).
[10] I. E. Grey *et al.*, J. Solid State Chem. **66**, 7 (1987).
[11] K. Fukuda *et al.*, Crystal Growth and Design **3**, 281 (2003).
[12] F. Sedona *et al.*, J. Phys. Chem. B **109**, 24 411 (2005).
[13] T. Matsumoto *et al.*, Surf. Sci. **572**, 127 (2004); **572**, 146 (2004).
[14] P. Fery, W. Moritz, and D. Wolf, Phys. Rev. B **38**, 7275 (1988); P. Fenter and T. Gustafsson, Phys. Rev. B **38**, 10 197 (1988).
[15] C. S. Fadley, in *Synchrotron Radiation Research, Advances in Surface and Interface Science*, edited by R. Z. Bachrach (Plenum, New York, 1992), Vol. 1, p. 421.
[16] J. P. Perdew, K. Burke, and M. Ernzerhof, Phys. Rev. Lett. **77**, 3865 (1996).
[17] D. Vanderbilt, Phys. Rev. B **41**, 7892 (1990).
[18] M. Lazzeri, A. Vittadini, and A. Selloni, Phys. Rev. B **63**, 155409 (2001).
[19] H. J. Monkhorst and J. D. Pack, Phys. Rev. B **13**, 5188 (1976).
[20] J. I. Lee, W. Mannstadt, and A. J. Freeman, Phys. Rev. B **59**, 1673 (1999); S. J. Jenkins, M. A. Petersen, and D. A. King, Surf. Sci. **494**, 159 (2001).
[21] J. Tersoff and D. R. Hamann, Phys. Rev. Lett. **50**, 1998 (1983).
[22] It is shown in the following that there is a strict relationship between anatase (001) and the actual phase obtained in the present case.
[23] Calculations on the full 14×4 system represent a formidable task, involving the treatment of slab models of $\sim$600 atoms.
[24] G. Granozzi and M. Sambi, Adv. Mater. **8**, 315 (1996).
[25] The rect-TiO_2 phase reported in Ref. [12] for titania on Pt (111) is actually a six-domain arrangement of lepidocrocite nanosheets.
[26] S. Surnev *et al.*, Phys. Rev. Lett. **87**, 086102 (2001); J. Schoiswohl *et al.*, Phys. Rev. Lett. **92**, 206103 (2004).
[27] S. Baroni *et al.*, QUANTUM ESPRESSO: opEn-Source Package for Research in Electronic Structure, Simulation, and Optimization. Code available from http://www.quantum-espresso.org.
[28] A. Kokalj, Comput. Mater. Sci. **28**, 155 (2003). Code available from http://www.xcrysden.org.